

BENDING RESPONSE OF HYBRID FERROCEMENT PLATES WITH MESHES AND FIBERS

Shuxin Wang* A. E. Naaman** Victor C. Li***

For ferrocement and laminated cementitious composites, increasing the number of mesh layers is not an efficient way to improve the modulus of rupture (MOR); moreover, at high reinforcement ratio severe spalling of matrix cover and delamination of extreme tensile layer are likely to lead to premature failure. Adding discontinuous fibers to the matrix provides a remedy to these drawbacks. In this paper, the bending response of hybrid ferrocement thin plates reinforced with meshes and fibers is reported and compared with conventional ferrocement composite with meshes and plain mortar. Three types of meshes, including two expanded steel meshes and one Kevlar FRP mesh, combined with two types of synthetic fibers, namely Spectra and PVA fibers, were experimentally investigated. The test results show that even at a high volume fraction of 6.73%, the expanded steel mesh can still be effectively used as reinforcement of ferrocement and a MOR exceeding 60 MPa was achieved. Compared with the specimens using plain mortar, the presence of fiber results in substantial increase in MOR, significant reduction in crack spacing and in turn crack width, prevention of cover spalling even at large deflection, and considerable improvement in shear capacity. An increase of the toughness and energy absorption to failure by up to 250% was also observed when a ductile fiber reinforced matrix was used with the FRP meshes. Non-linear analysis was employed to predict the MORs of the composites, and good agreement was observed.

Keywords: bending, expanded steel mesh, FRP mesh, fiber, MOR

INTRODUCTION

Ferrocement is a type of thin wall reinforced concrete commonly constructed of hydraulic cement mortar reinforced with closely spaced layers of continuous and relatively small size wire mesh [1]. In its role as a thin reinforced concrete product and as a laminated cement-based composite, ferrocement has found itself in numerous applications both in new structures and repair and rehabilitation of existing structures. Compared with the conventional reinforced concrete, ferrocement is reinforced in two directions; therefore, it has homogenous-isotropic properties in two directions. Benefiting from its usually high reinforcement ratio, ferrocement generally has a high tensile strength and a high modulus of rupture. In addition, because the specific surface of reinforcement of ferrocement is one to two orders of magnitude higher than that of reinforced concrete, larger bond forces develop with the matrix resulting in average crack spacing and width more than one order of magnitude smaller

* Graduate Student Research Assistant, Dept. of Civ. & Env. Engrg., Univ of Michigan, Ann Arbor, USA.

** Professor, Dept. of Civ. & Env. Engrg., Univ of Michigan, Ann Arbor, USA.

*** Professor, Dept. of Civ. & Env. Engrg., Univ of Michigan, Ann Arbor, USA.

than in conventional reinforced concrete [2-3]. Other appealing features of ferrocement include ease of prefabrication and low cost in maintenance and repair. Based on the aforementioned advantages, the typical applications of ferrocement include water tanks, boats, housing wall panel, roof, formwork and sunscreen [4-6].

The renaissance of ferrocement in recent two decades has led to the ACI design guideline "Guide for the Design, Construction, and Repair of Ferrocement, [7], and publications such as "Ferrocement Design, Techniques, and Application" [8] and "Ferrocement and Laminated Cementitious Composites, [9], which provide comprehensive understanding and detailed design method of contemporary ferrocement. However, the rapid development in reinforcing meshes and matrix design requires continuous research to characterize the new material and improve the overall performance of ferrocement. Thus far steel meshes have been the primary mesh reinforcement for ferrocement, but recently fiber reinforced plastic (FRP) meshes were introduced in ferrocement as an promising alternative to steel meshes [1 -14]. Compared with steel, FRP materials possess some remarkable features such as lightweight, high tensile strength and inherent corrosion resistance. However, unlike steel that has an elastic-plastic stress-strain relationship, FRP materials behave elastically up to failure, thus do not yield and lack ductility. To prevent brittle tensile flexural failure, FRP reinforced members are usually designed to be over-reinforced and thus the nonlinear deformation capacity as well as the strain-softening region of concrete matrix could be utilized. In fact, the over-reinforced condition is intrinsically satisfied for the range of reinforcement ratio used in practice [15], in particular for thin ferrocement plates.

As a laminated composite, ferrocement often suffers from severe spalling of matrix cover and delamination of extreme tensile layer at high reinforcement ratio, resulting in premature failure. Therefore, serviceability consideration rather than strength limit would dominate composite design. Adding discontinuous short fiber to cementitious matrix, which could bring significant improvement in ductility and shear capacity as well as moderate increase in tensile strength, turns out to be a logical solution to solve or alleviate these problems.

In this paper, investigation on ferrocement thin plates reinforced by two types of low cost expanded steel meshes and one Kevlar FRP mesh, as well as two types of synthetic discontinuous short fibers, namely Spectra and PVA fibers, are reported. Results of the control specimen without fiber are also presented for comparison. MORs were further predicted by theoretical models, and good agreement was observed.

EXPERIMENTAL PROGRAM

The main parameters investigated in this project include the type of mesh, the volume fraction of reinforcement and the addition of discontinuous fibers. Two types of gage 20 expanded steel meshes and one type of Kevlar FRP mesh were studied. The steel meshes both have a thickness of 0.76mm, and one has an opening of 25.4mm (1") in longitudinal direction (ES 1 see Fig. 1(a)) while the other has an opening of 12.7mm (0.5") (ES 2, see Fig. 1(b)). For expanded meshes, only the longitudinal direction is used as the reinforcing direction. Direct tensile tests on coupons of steel taken from the mesh showed that these two meshes have different yield strengths. Figure 1 (c) shows the picture of the Kevlar mesh used in this study.

The fabric style has 10x6 fiber-bundles per square inch, i.e., a spacing of about 2.5 mm in the longitudinal direction and 3.5 mm in the transverse direction, and a yarn of 1500 denier in each direction. In the longitudinal direction, the yarn has a "leno" twist. The mechanical properties of the meshes are listed in Table 1. Two types of polymeric fibers, namely PE Spectra 900 fiber and Poly Vinyl Alcohol (PVA) fiber, are investigated in combination with different mesh reinforcements; their properties are given in Table 2. Two types of matrices with a compressive strength about 75 MPa were used; mix

proportions are given in Table 3. Since the reinforcement ratio was relatively high for all the specimens, high strength matrix was chosen to improve the bending ductility.

Eight series totaling 24 ferrocement plate specimens were prepared and tested under four-point bending. The specimens measure 304.8mm(L) x 76.2mm(W) x 12.7mm(H). The combinations of mesh, matrix, and fiber for these specimens are tabulated in Table 3. The first three series are the control specimens without short fibers; series 4, 5, and 6 contain 2 layers of steel mesh and fibers; series 7 and 8 contain two layers of Kevlar mesh and fibers, the difference between the two series is the loading direction of the mesh.

For hybrid composites with mesh and discontinuous fiber, a horizontal casting mold was used, whereas the specimens without fiber were cast vertically. The two extreme mesh layers were placed close to the surface of the mold with a cover of about 1.5 rom. Other layers, when present, were distributed at best in between. Moderate vibration was applied when casting. All the specimens were demolded 24 hours after casting, then stored in water tank until the day before testing. The age at testing was about 12 to 14 days. All specimens were tested under four- point bending with a span of 228.6 mm. Tests were conducted on a MTS 810 frame system with a load capacity of 100 kN. The mid-span deflection was monitored by an external LVDT .

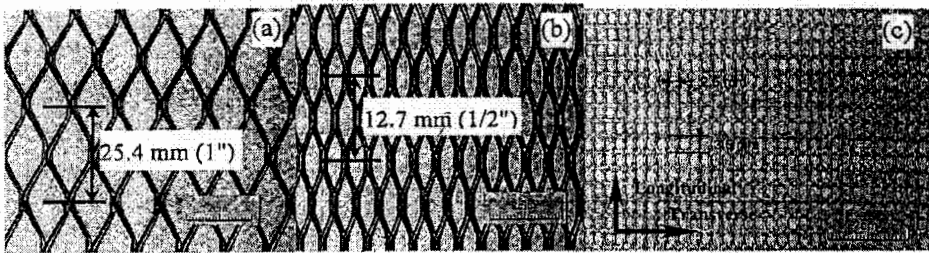


Fig. 1 – (a) Expanded Steel Mesh ES1 with 25.4mm (1") Opening
 (b) Expanded Steel Mesh ES2 with 12.7mm (1/2") Opening
 (c) Kevlar Mesh, 1500 Denier per Yarn

Table 1 – Mesh Properties

Mesh Name	Tensile Strength (MPa)	Effective Modulus E_r (GPa)		Efficiency Factor		Ultimate Elongation (%)
		E_{rL}	E_{rT}	η_L	η_T	
ES1 ⁽¹⁾	307	138	69	0.65	0.20	N.A.
ES2 ⁽²⁾	410	138	69	0.65	0.20	N.A.
Kevlar	2800	124		0.625	0.375	2.8%

(1) Expanded Steel Mesh with 25.4mm (1") Opening.

(2) Expanded Steel Mesh with 12.7mm (1/2") Opening.

Table 2 – Fiber Properties

Fiber Type	Length (mm)	Diameter (μm)	Modulus (GPa)	Tensile Strength (MPa)
Spectra 900	19	38	120	2400
PVA 1	12	190	29	900
PVA 2	6	14	29	900

Table 3 – Summary of Specimens

Series	Matrix	Mesh Type	Number of Layers	Mesh V_f	$V_{ft}^{(1)}$	Fiber V_f	$V_f + V_{ft}$
No. 1	Mix 1	ES1	2	3.37%	2.19%	No	3.37%
No. 2	Mix 1	ES1	4	6.73%	4.37%	No	6.73%
No. 3	Mix 1	ES2	2	6.73%	4.37%	No	6.73%
No. 4	Mix2	ES1	2	3.37%	2.19%	PE 1.5%	4.87%
No. 5	Mix2	ES2	2	6.73%	4.37%	PE 1.5%	8.23%
No. 6	Mix2	ES1	2	3.37%	2.19%	PVA1 2%	5.37%
No. 7	Mix2	Kevlar Mesh L Direction	2	1.15%	0.72%	PE 1.5%	2.65%
No.8	Mix2	Kevlar Mesh T Direction	2	1.15%	0.43%	PE 1.5%	2.65%

(1) Assuming $\eta_L = 0.65$ **Table 4 – Matrix Proportions**

Matrix No.	Cement ⁽¹⁾	Sand ⁽²⁾	Water	Strength (MPa)
Mix1	1	1	0.36 ⁽³⁾	77
Mix2	1	0.5	0.28 ⁽⁴⁾	74

(1) Type I Portland cement.

(2) Fine silica sand 50/70.

(3) 2 wt% of Superplasticizer was added.

(4) 3 wt% of Superplasticizer was added.

TEST RESULT AND DISCUSSION

The results of four-point bending tests are presented in the form of equivalent bending stress vs. mid-span deflection curves, which represent the average of three test specimens.

Effect of Increasing Number of Layers vs. 2 Layers of Same Volume Fraction

For ferrocement with plain mortar there are two means to improve the modulus of rupture (MOR), i.e., increasing the number of mesh layers and using a mesh of higher volume fraction. Series 1 contains 2 layers of mesh ES1 with 25.4 mm opening, and series 2 and 3 have doubled mesh volume fraction as that of series 1. The difference between the latter two is that series 2 has 4 layers of mesh ES 1 while series 2 uses 2 layers of mesh ES2 with 12.7 mm opening. As shown in Fig.2, the MOR of series 2 is about 80% higher than that of series 1 and that of series 3 is almost three times that of series 1. Moreover, the bending stiffness of series 3 is significantly higher than that of series 2 prior to mesh yielding. This is because, everything else being equal, placing all the reinforcement in the extreme layers is more efficient than distributing it evenly throughout the depth. In addition, the yielding strength of the mesh ES2 was higher than that of the mesh ES 1.

Photos showing ultimate states of these specimens are given in Fig. 3 to 5. Severe matrix spalling can be clearly seen. Series 1 behaved in a very ductile manner and failed in flexural tension, while series 2 failed in flexural compression and the ductility thus deteriorated. Mesh rupture of the tensile layer was observed in both series at ultimate state. However, for series 2, flexural compression failure occurred prior to tensile rupture of mesh, indicating the specimen is over-reinforced. Similarly to series 2, the matrix of series 3 crushed at about the stage of strain- hardening of the mesh, leading to a slight drop in load. For ferrocement plates under bending, usually only one extreme layer is subjected to compression. After compression failure of the matrix, which is very likely to happen under large plastic rotation, substantial resistance to compression has to be provided by the extreme layer of mesh in the compression zone. Series 3 has a higher ratio of compression reinforcement than series 2, and therefore exhibited a significantly higher ductility. Series 3 finally failed in the delamination of the extreme layer of tensile mesh induced by horizontal shear.

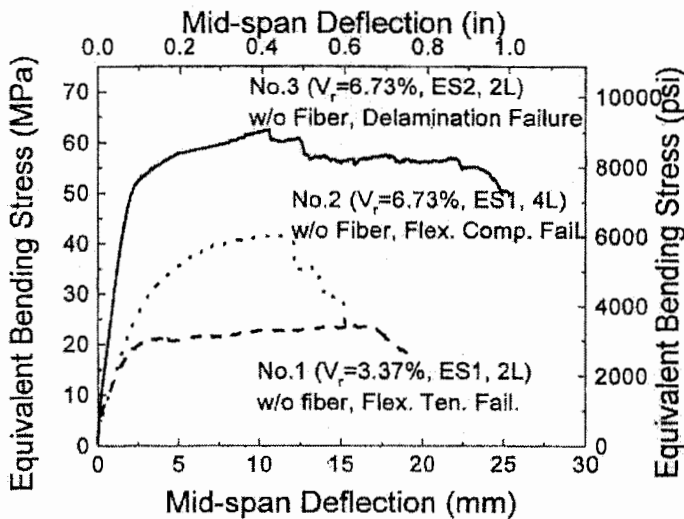


Fig. 2. Average Stress-Deflection Curves of Series 1 to 3



Fig. 3. Ultimate State of Specimen Series 1
(4 Layers of Mesh ES1, w/o fiber)

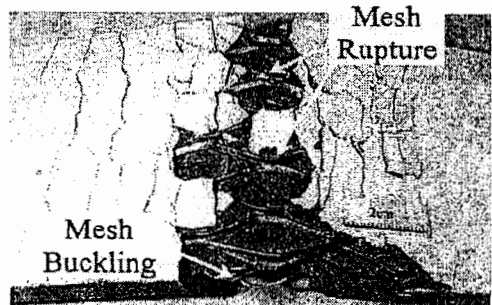


Fig. 4. Ultimate State of Specimen Series 2
(2 Layers of Mesh ES1, w/o fiber)

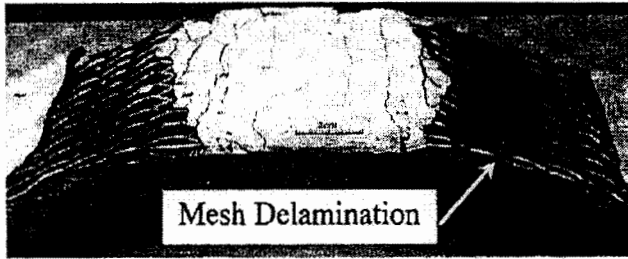


Fig. 5. Ultimate State of Specimen Series 2
(2 Layers of Mesh ES2, w/o fiber)

Effect of Adding Fibers

Plain mortar matrix was replaced with fiber reinforced cementitious composites (FRCC) in series 4 through 8. Two types of discontinuous fibers, PE Spectra fiber and PVA fiber, were used with a volume fraction of 1.5% and 2.0%, respectively. The PE Spectra fiber combined with the specially designed matrix (Mix 2) is also known as an Engineered Cementitious Composite (ECC). ECC is a category of high performance fiber reinforced cement composite (HPFRC) designed based on micromechanical models. Unlike conventional FRCCs, ECC features significant strain-hardening and multiple cracking behavior. Its tensile strain can reach as high as 6% with an ultimate tensile strength of 5 MPa [6]. On the other hand, the PVA-FRC, at the compressive strength considered, may be classified as a conventional FRC with tension-softening behavior. Note that the compressive strengths of the PE-ECC and PVA-FRC were very close, providing a better baseline for comparison.

Hybrid Composites with Steel Meshes and Discontinuous Fibers

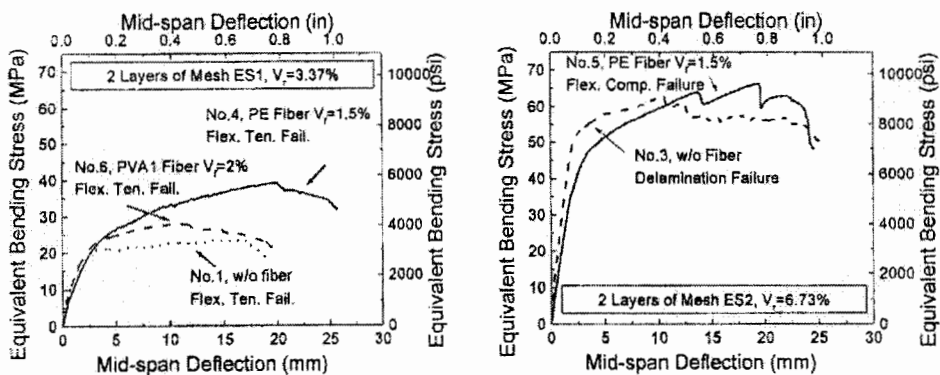


Fig. 6. Average Stress-Deflection Curves of Ferrocement Plates with Expanded Steel Mesh and Discontinuous Fibers

Expanded steel mesh ES 1 and ES 2 were used in series 4 to 6. The comparison with the series without fiber was illustrated in Fig. 6. Series 4 has same mesh layout as series 1 except for the ECC matrix with fibers; its bending performance was very different. Significant improvement was observed in terms of MOR, ductility, fracture energy and the crack pattern. As shown in Fig. 7, numerous fine cracks developed, and no matrix spalling was observed. The specimens finally failed in tension with 64 % improvement in MOR (39.3 MPa) compared with counterpart specimen series 1 (23.9 MPa). However, for series 6 that is the equivalent specimen with PVA-FRC matrix, the improvement is only marginal compared with series 1, even though higher fiber volume fraction is used than that of series 4. This manifests the importance of proper design and optimization of the fiber reinforced cementitious matrix. As shown in Fig. 9, the crack spacing of series 6 is much larger than that of series 4 (Fig. 7), but still smaller than that without fibers (Fig. 4). The presence of fibers effectively prevents the spalling of matrix. In general, the modulus of elasticity of polymeric fibers is much lower than that of steel mesh; thus the addition of such fibers does not noticeably influence the composite bending behavior before yielding of the mesh. However, with the increase of crack opening, the contribution of the bridging force due to the fibers becomes significant. Thus the improvement of bending strength due to the fibers is usually observed at the post-yielding stage. Moreover, this improvement strongly depends on the fiber and interface properties, as well as the fiber volume fraction. For instance, when a high ratio of mesh reinforcement is used, the increase of MOR due to the presence of fibers becomes marginal, as illustrated by the comparison between the specimens of series 5 and series 2. Both of them have two layers of 1/2 in. expanded mesh ($V_f = 6.73\%$), and their matrix crushes at the stage of mesh strain-hardening. Recognizing that the addition of fibers has little influence on the compressive strength, it is not surprising that the MOR of these two specimens is very close. However, this does not mean that for over-reinforced specimens there is no advantage in adding fibers. Indeed, besides the significant improvement in crack spacing and width, and the prevention of cover spalling, the addition of discontinuous fibers considerably increases the shear resistance of the matrix, and therefore, effectively delays the delamination of the extreme layer of tensile mesh (Fig. 8).

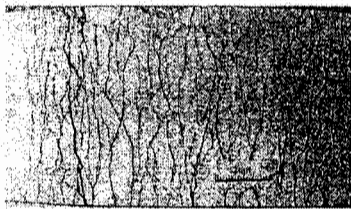


Fig. 7— Ultimate State of Specimen Series 4 (2 Layers of ES1 with Spectra fiber $V_f=1.5\%$)

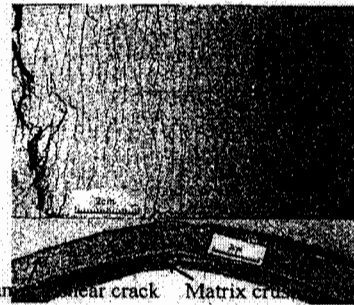


Fig. 8— Ultimate State of Specimen Series 5 (2 Layers of ES2, with Spectra fiber $V_f=1.5\%$)



Fig. 9— Ultimate State of Specimen Series 6 (2 Layers of Mesh ES1, with PVA fiber $V_f=2.0\%$)

Table 5 Toughness Index of Series with Expanded Steel Mesh

Series	Description	Toughness Index
No. 1	2 Layers of Mesh ES1	88.4
No. 2	4 Layers of Mesh ES1	81.9
No. 3	2 Layers of Mesh ES2	542
No. 4	2 Layers of Mesh ES1 + 1.5% PE Fiber	123
No. 5	2 Layers of Mesh ES2 + 1.5% PE Fiber	548
No. 6	2 Layers of Mesh ES1 + 2.0% PVA1 Fiber	110

Table 5 lists the toughness index of series 1 to 6, which is defined as the ratio of the area under the stress-deflection curve up to a given deflection to the area under the curve up to the deflection at cracking [17]. The numerator of the index can be considered as the total energy up to the given deflection, which is set to 20mm except for series 2 where the peak point is used; the denominator can be considered as the elastic energy where the cracking stress is arbitrarily assumed as 10MPa. These indices clearly provide better understanding of the role of fiber in improving composite toughness. For the series with 2 layers of mesh ES 1, which is considered at relatively low reinforcement ratio, the addition of fiber significantly contributes to the improvement of composite toughness; while at high reinforcement ratio (series 3 and 5) the toughening effect of fiber becomes marginal

Hybrid Composites with Kevlar Mesh and Discontinuous Spectra Fibers

Two series (7 and 8 of Table 3) of specimens reinforced with same Kevlar fiber mesh but in different direction were tested. PE-ECC was used as matrix since previous tests showed that with a plain mortar matrix the specimen always failed by delamination of the extreme tensile layer of mesh [13]. The average equivalent bending stress versus deflection curves are presented in Fig. 10 and compared with other control tests [3]. It is observed that the two series (7 and 8) reinforced with the same Kevlar mesh but oriented in either the longitudinal or the transverse direction, behave very similarly. After first cracking, they exhibit almost linear behavior due to the elastic nature of the FRP material, followed by compressive failure of the matrix. However, the crushing of PE-ECC matrix is rather gradual while maintaining a high resistance, and a very good composite ductility is observed. MaR values higher than 40 MPa were achieved for these specimens at a large deflection of 35 mm.

For series 7 and 8, the balanced reinforcement ratio, which produces a simultaneous failure both by tensile rupture of FRP mesh and compression crushing of the matrix, can be calculated from the following equation:

$$\rho_b = \frac{0.85\beta_1 f'_c}{\sigma_{fc}} \left(\frac{\epsilon_{cu}}{\epsilon_{cu} + \epsilon_{fc}} \right) \dots\dots\dots(1)$$

where $\beta_1 = 0.65$; f'_c and ϵ_{cu} are the compressive strength and strain of matrix respectively; σ_{fc} and ϵ_{fc} are the tensile strength and ultimate strain of FRP mesh respectively. Using $\epsilon_{cu} = 0.0050$ for PE-ECC and other values available in Table 4, ρ_b is equal to 0.221 %. The tensile reinforcement ratios of series 7 and 8 are 0.36% (longitudinal direction, series 7) and 0.215% (transverse direction, series 8) respectively; both are higher than the balanced reinforcement ratio. Therefore, compression

failure of the matrix would occur first. Since compressive failure of matrix controls, the difference in reinforcement ratio between these two series does not significantly influence the bending strength. Finally, note that the addition of fibers may significantly improve the compressive strain at failure of the matrix and the shape of the stress- strain curve in compression, thus leading to significant improvement in composite ductility even when over-reinforced.

Fig. 11 shows the ultimate state of a typical specimen from series 7, which is also quite similar to that of series 8. Very fine parallel cracks are observed. These cracks can be categorized into two groups: primary cracks and secondary cracks. The primary cracks have a spacing of about 3-4 mm, which corresponds approximately to the spacing of the transverse yarn of mesh, and is probably initiated by the presence of the transverse yarns. Between these primary cracks, one can observe one or two filler cracks. These secondary cracks are generated by the bond shear stress transfer at the matrix-mesh interface, and close after unloading due to the elastic behavior of Kevlar mesh. The delamination of the tensile layer at the final stage of loading, can still be observed in the figure; however, compared with the control specimens without fibers, in which the interlaminar shear failure is often the controlling limit state, this failure mode is significantly delayed by the presence of the fibers. A similar observation is also made with the specimens using PVA fibers. However, the specimens with 1.5% Spectra fiber exhibited much better ductility.

Another interesting observation is that although the tensile reinforcement ratio is significantly different when using different direction of this Kevlar mesh ($V_{rt}=0.72\%$ vs. $V_{rt}=0.42$) the corresponding bending stiffness is almost same. One plausible explanation is that although the yarn in the longitudinal direction is denser than that in the transverse direction, its 'reno' twist leads to a reduction in the effective stiffness of the mesh.

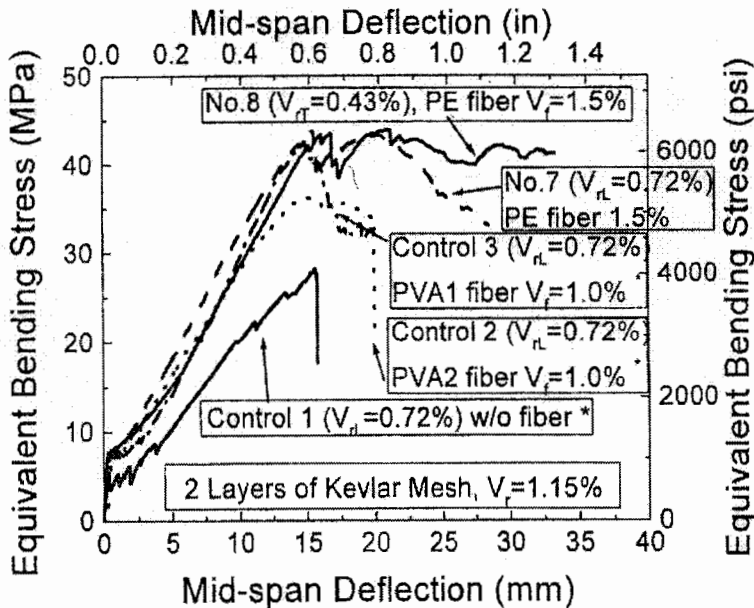


Fig. 10. Average Stress-Deflection Curves of Hybrid Ferrocement with 2 Layers of Kevlar Mesh and Discontinuous Fibers (* see ref [13])

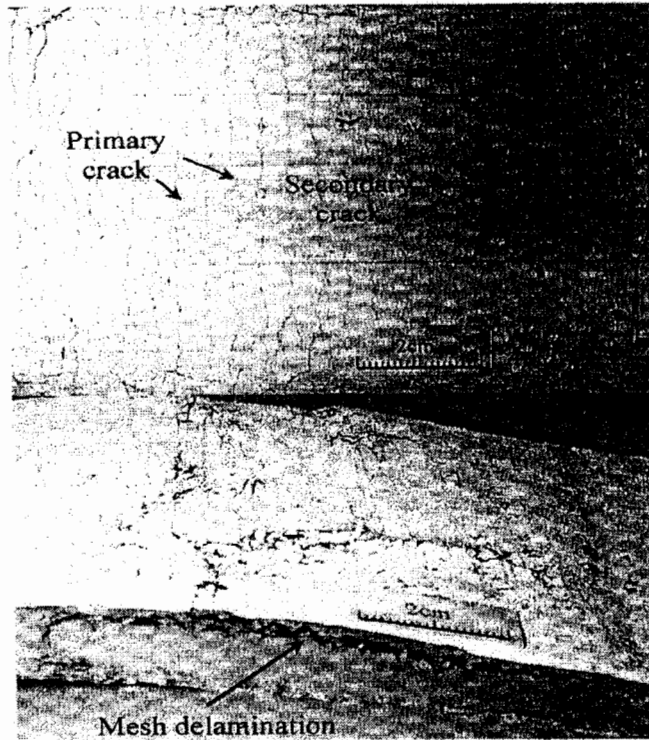


Fig. 11. Ultimate State of the Hybrid Composite with Kevlar Mesh and Spectra Fiber (Mesh is in Longitudinal Direction.)

For better comparison of the toughening effect of different fibers to the composite plates with Kevlar mesh, a toughness ratio is defined. Herein the area under the stress-deflection curve of series Control 1, which does not contain fiber, is defined as the reference. The ratio of the area under the curve of other series with fiber to this reference is tabulated in Table 6, which clearly indicates the toughening effect of the addition of fiber. The toughness series 8 is almost four times of that without fiber.

Table 6 Toughness Index of Series with Kevlar Mesh

Series	Composition Description	Toughness Ratio
Control 1	2 Layers, L Direction, No Fiber	1.0
Control 2	2 Layers, L Direction, 1.0% PVA2 Fiber	2.0
Control 3	2 Layers, L Direction, 1.0% PVA1 Fiber	2.1
No. 7	2 Layers, L Direction, 1.5% PE Fiber	3.7
No. 8	2 Layers, T Direction, 1.5% PE Fiber	3.9

Overview of Crack Spacing and MOR

Fig. 12 provides a summary of the average MaR and crack spacing values observed for the eight series of tests undertaken (Table 3). Also shown is the total volume fraction of reinforcement (that is due to the mesh and fibers) of the composite. The following observations can be made. First, with an increase in reinforcement ratio of same mesh, the MOR increases and the crack spacing (thus crack width) decreases. Second, compared with the same specimen using plain mortar, the addition of discontinuous fibers to the matrix can effectively increase the MOR and significantly reduce the crack spacing and width. Finally, hybrid composites with 2 layers of Kevlar mesh ($V_r=1.15\%$) and 1.5% Spectra fibers (series No.7) achieve respectively, almost same MOR and a crack spacing about one fifth that of specimens with 4 layers of expanded steel mesh (No.2, $V_r=6.73\%$). Figure 14 suggests that there is some optimizing and trade-off to do to determine the hybrid combination that leads to the best properties and the least consumption of total reinforcement, or the least cost.

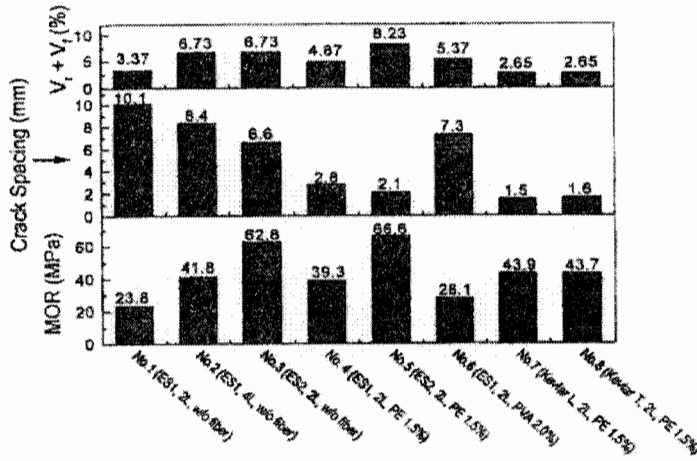


Fig. 12. Comparison of MOR and Crack Spacing for Different Total Volume of Reinforcement

PREDICTION OF MOR

The moment capacity and the MOR of the expanded steel mesh reinforced ferrocement plates can be calculated by the simplified method based on all tensile reinforcement yielding [9]. For the specimens with discontinuous fibers, the bridging force contributed by the fibers in the tensile zone should be considered. Here only specimens with PE-ECC are considered. Since the PE-ECC undergoes strain-hardening in tension, a uniform tensile stress distribution as shown in Fig. 13 is assumed for simplicity; f'_c is the compressive strength of PE-ECC, b is the plate width, σ_{fc} is average tensile strength of PE-ECC (5 MPa), h is the yielding strength of steel mesh, A_r is the reinforcement area. Assuming there is only one layer of tensile mesh and writing the force and moment equilibrium equations, the depth of rectangular block a and the moment capacity M can be calculated from Eqs. 2 and 3. Predicted and experimentally observed MOR are compared in Table 7; a good agreement is observed.

For the hybrid composite with Kevlar mesh and PE fiber, the calculation becomes more complicated. Because the section is over-reinforced and the mesh is linearly elastic, strain compatibility has to be considered. Herein, nonlinear analysis based on strain compatibility is used to predict the equivalent bending stress versus mid-point deflection relationship. The force and moment equilibrium equations are solved in incremental steps by numerical methods. The Kevlar mesh is assumed linear elastic with a Young modulus of 124 GPa; the tensile and compressive stress-strain curves of PE-ECC measured from uniaxial tension and compression tests are input as material constitutive laws. Since the yarn in longitudinal direction has a "leno" twist and the effective modulus is unknown, only the plate reinforced by the transverse direction of Kevlar mesh is calculated. After obtaining the moment-curvature relationship, the deflection is computed by simple beam theory. Fig. 14 compares the predicted curve and the experimental curves. A relatively good agreement is observed.

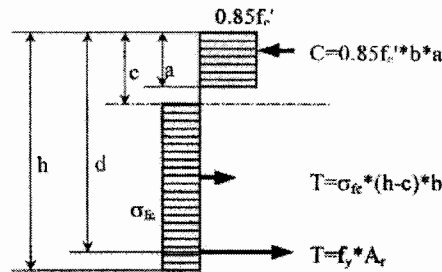


Fig. 13 – Stress Distribution at the Cross-Section of Hybrid Composite with Steel Mesh and Fiber

$$a = \beta_1 \frac{\sigma_k b h + f_y A_r}{0.85 \beta_1 f_c' b + \sigma_k b} \tag{2}$$

$$M = A_r f_y (d - a/2) + \sigma_k (h - c) b (h/2 + c/2 - a/2) \tag{3}$$

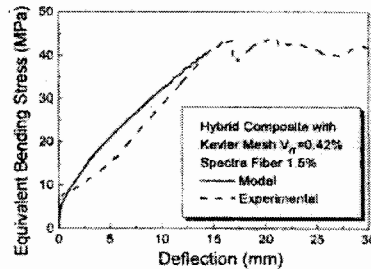


Fig. 14 – Comparison between the Predicted and Experimental Stress-Deflection Relationship

Table 7 Comparison of Predicted MOR and Experimental Result

Series	Experimental (MPa)	Prediction (MPa)
No.1 (ES1, 2L, w/o fiber)	23.3	23.8
No.2 (ES1, 4L, w/o fiber)	42.6	41.8
No.3 (ES2, 2L, w/o fiber)	63.4	62.8
No. 4 (ES1, 2L, PE fiber)	39.9	39.3
No. 8 (Kevlar T, 2L, PE fiber)	41.2	43.7

CONCLUSION

The following observations and conclusions are drawn from this study:

1. Expanded steel mesh can be effectively used as reinforcement for ferrocement. Good ductility and modulus of rupture exceeding 60 MPa were achieved for a total volume fraction of mesh of 6.73%.
2. Increasing the volume fraction of reinforcement leads to an increase in MOR and a decrease in average crack spacing and width.
3. Everything else being equal, the addition of discontinuous fibers to the matrix of ferrocement can effectively increase its MOR and significantly reduce the average crack spacing and width at ultimate loading. Moreover, the presence of fibers improves the shear capacity of the matrix and thus delays the interlaminar shear failure that is likely to occur at high reinforcement ratios.
4. The addition of fibers to the matrix can be very effective in preventing the spalling of the mortar cover at ultimate load.
5. Hybrid composites with 2 layers of Kevlar mesh ($V_r = 1.15\%$) and 1.5% Spectra fibers achieved respectively, almost same MaR and one fifth the crack spacing as specimens with 4 layers of expanded steel mesh with $V_r = 6.73\%$.
6. When PE Spectra fibers were used at 1.5% volume fraction, ductile failure mode was observed in Kevlar mesh reinforced specimens rather than the brittle interlaminar shear failure usually observed with FRP mesh reinforced composites.
7. Everything else being equal, the addition of fiber to ferrocement plates with only 2 layers of mesh increases their toughness indices from 2 times to 3.9 times.

REFERENCES

1. ACI Committee 549, "State-of-the-Art Report on Ferrocement", ACI 549-R97, in Manual of Concrete Practice, ACI, Detroit, 1997, 26pp.
2. Shah, S.P and Naaman, A.E., "Crack Control in Ferrocement and Its Comparison with Reinforced Concrete," Journal of Ferrocement, V. 8, No.2, pp.67-80.
3. Naaman, A.E. and Shah, S.P., "Tensile Test of Ferrocement," ACI Journal, Proceedings, V. 68, No. 9, Sept., 1971, pp. 693-698.
4. Guerra, A.E., Naaman, A.E. and Shah, S.P., "Ferrocement Cylindrical Tanks: Cracking and Leakage Behavior," ACI Journal, Proceedings, V. 75, No.1, Jan., 1978, pp. 22-30.

5. Nimityongskul, P., Chen Bor-Shiun and Karasudhi, P., "Impact Resistance of Ferro cement Boat Hulls," Journal of Ferro cement, V.10, No.1, 1980, pp. 1.10.
6. Kadir, M.R.A., Samad, A.A.A., Muda, I.C., and Abang Abdullah, A.A., "Flexural Behavior of Composite Beams with Ferro cement Permanent Formwork," Journal of Ferro cement, V. 27, No.3, 1997, pp. 209-214.
7. ACI Committee 549-1R-88, "Guide for Design Construction, and Repair of Ferro cement" ACI 549-1R-88 and 1R-93, in Manual of Concrete Practice, ACI, Detroit, 1993, 27pp.
8. Bingham, B., *Ferro-cement Design, Techniques, and Applications*, Cornell Maritime Press, Cambridge, Maryland, 1974, 444pp.
9. Naaman, A., *Ferro cement and Laminated Cementitious Composites*, Techno Press 3000, Ann Arbor, Michigan, 2000, 372pp.
10. Naaman, A.E., and Al-Shannag, J. "Ferro cement with Fiber Reinforced Plastic Meshes: Preliminary Investigation," Proceedings of the Fifth International Symposium on Ferro cement, Manchester, England, September 1994. P. Nedwell and N.R. Swamy, Editors, E. and FN SpaN, London.
11. Guerrero, P. and Naaman, A. E., "Bending Behavior of Hybrid Ferro cement Composites Reinforced with PV A Meshes and PV A Fibers," Ferro cement 6 -Lambot Symposium, Proceedings of Sixth International Symposium on Ferro cement, Naaman, A.E., Editor, University of Michigan, June 1998.
12. Naaman, A.E., and Guerrero, P., "Bending Behavior of Thin Cement Composites Reinforced with FRP Meshes," Proceedings of First International Conference on Fiber Composites in Infrastructures, ICCI 96, Edited by H. Saadatmanesh and M. Ehsani, University of Arizona, Tucson, January 1996, pp. 178-189.
13. Naaman, A.E., and Chandrangsou, K., "Bending Behavior of Laminated Cementitious Composites Reinforced with FRP Meshes," High Performance Fiber Reinforced Concrete Thin Sheet Products, Edited by A. Peled, S.P. Shan and N. Banthia, ACI SP-190, American Concrete Institute, Farmington Hills, 2000, pp. 97-116.
14. Lopez, M. and Naaman, A. E., "Study of Shear Joints in Fiber Reinforced Plastic (FRP) Ferro cement Bolted Connections," Ferro cement 6 -Lambot Symposium, Proceedings of Sixth International Symposium on Ferro cement, Naaman, A.E., Editor, University of Michigan, June 1998.
15. Nanni, A., "Flexural Behavior and Design of RC Members Using FRP Reinforcement," Journal of Structural Engineering, V. 119, No. 11, Nov. 1993, pp. 3344-3359.
16. Li, V. C., "From Micromechanics to Structural Engineering -The Design of Cementitious Composites for Civil Engineering Application." JSCE J: of Structural Mechanics and Earthquake Engineering, V.10, No.2, 1993, pp. 37-48.
17. Naaman, A. E. and Reinhardt, H. W., "Characterization of High Performance Fiber Reinforced Cement Composites -HPFRCC." Proceeding of the RILEMIACI Workshop: High Performance Fiber Reinforced Cement Composites. Naaman, A. E. and Reinhardt, H. W., Editors, London: E&FN SpaN, 1995. p.1-23.